

# We are IntechOpen, the world's leading publisher of Open Access books Built by scientists, for scientists

**4,800**

Open access books available

**122,000**

International authors and editors

**135M**

Downloads

Our authors are among the

**154**

Countries delivered to

**TOP 1%**

most cited scientists

**12.2%**

Contributors from top 500 universities



**WEB OF SCIENCE™**

Selection of our books indexed in the Book Citation Index  
in Web of Science™ Core Collection (BKCI)

Interested in publishing with us?  
Contact [book.department@intechopen.com](mailto:book.department@intechopen.com)

Numbers displayed above are based on latest data collected.

For more information visit [www.intechopen.com](http://www.intechopen.com)



---

# Optimization of the Synthesis Procedures of Graphene and Graphite Oxide

---

María del Prado Lavín López,  
José Luis Valverde Palomino,  
María Luz Sánchez Silva and  
Amaya Romero Izquierdo

Additional information is available at the end of the chapter

<http://dx.doi.org/10.5772/63752>

---

## Abstract

The optimization of both the *chemical vapor deposition (CVD)* synthesis method to prepare graphene and the *Improved Hummers method* to prepare graphite oxide is reported. Copper and nickel were used as catalysts in the CVD-graphene synthesis, CH<sub>4</sub> and H<sub>2</sub> being used as precursor gases. Synthesis variables were optimized according to a *thickness value*, calculated using a homemade Excel-VBA application. In the case of copper, the maximum *thickness value* was obtained for those samples synthesized at 1050°C, a CH<sub>4</sub>/H<sub>2</sub> flow rate ratio of 0.07 v/v, a total flow of 60 Nml/min, and a time on stream of 10 min. In the case of nickel, a reaction temperature of 980°C, a CH<sub>4</sub>/H<sub>2</sub> flow rate ratio of 0.07 v/v, a total flow of 80 Nml/min, and a time on stream of 1 min were required to obtain a high *thickness value*. On the other hand, the *Improved Hummers method* used in the synthesis of graphite oxide was optimized. The resultant product was similar to that reported in literature in terms of quality and characteristics but both time and cost of the synthesis procedure were considerably decreased.

**Keywords:** graphene, graphite oxide, CVD, Improved Hummers method, thickness value

---

## 1. Introduction

Carbon (C) is a chemical element with atomic number 6 and solid at room temperature. Depending on the synthesis conditions during its growth, carbon can be found in nature with

---

different allotrope forms [1]. Among them, the softer and the harder materials known in nature are included: graphite (**Figure 1a**) and diamond (**Figure 1b**), respectively. Recently, new carbon allotropes have been discovered such as fullerenes (**Figure 1c**), carbon nanotubes (**Figure 1d**), carbon nanofibers (**Figure 1e**), and carbon nanospheres. To date, the last carbon allotrope that has been appended is graphene (**Figure 1f**). It consists of a two-dimensional (2D) carbon atom network with  $sp^2$  hybridization and only one atom thick [2]. Each atom is bonded by a covalent bond to other three carbon atoms. These carbon atoms are densely packed in a honeycomb-shape crystal lattice [3] comprising, in turn, of two superimposed triangular subnets [4]. Although graphene has been known since 1960, it was not until 2004 when Andre Geim and Konstantin Novoselov achieved to obtain an isolated graphene sheet using the Scotch<sup>®</sup> tape method [5].



**Figure 1.** Structure of (a) graphite, (b) diamond, (c) fullerene, (d) carbon nanotube (CNT), (e) carbon nanofiber (CNF), and (f) graphene [6].

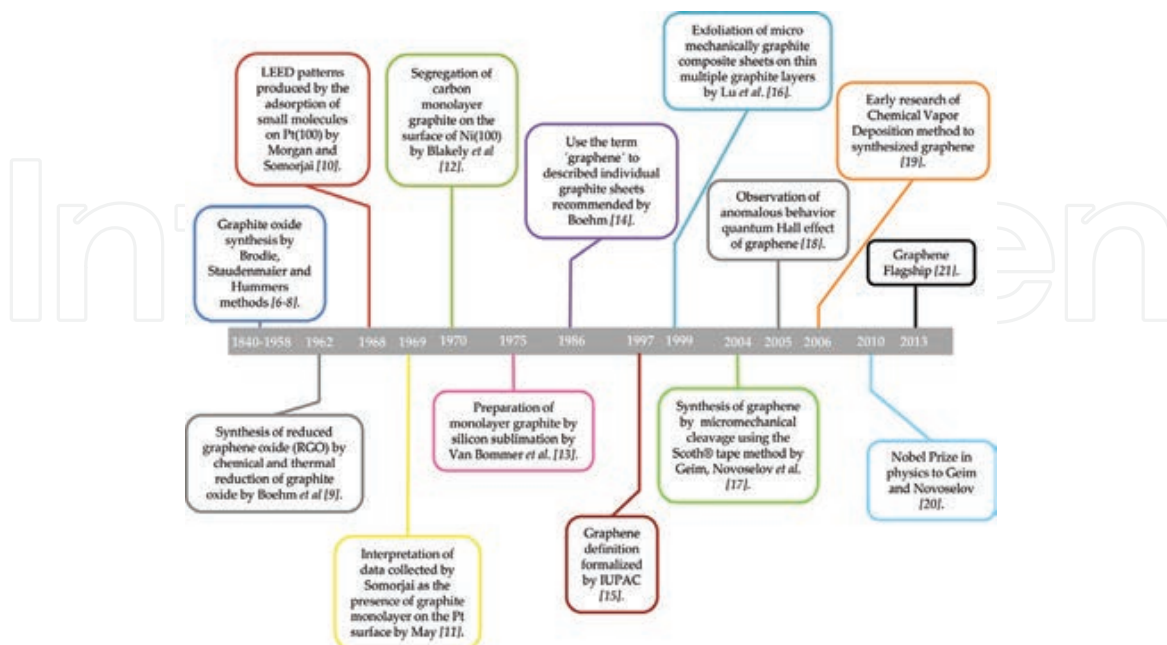


**Figure 2.** Roadmap of graphene [5, 7–21].

## 1.1. Graphene chronology

Graphene is one of the most extensively researched materials and is currently regarded as a fascinating material [2]. **Figure 2** shows the chronology of graphene, from 1840 to nowadays.

## 1.2. Properties and applications

Since 2004, many researchers have been focused on the synthesis of high-yield and high-quality graphene as well as on the search of an easily scalable process to manufacture it [6]. **Table 1** shows the extraordinary properties of graphene related to the applications that can be derived from them.

| Property   | Application  | Ref.    |
|--|--|---------|
| • High-speed electron mobility                                     | Transistors, lasers, photo detectors                         | [3, 22] |
| • Large specific surface area                                      | Sensors  | [2, 23] |
| • Conductance  |  |         |
| • Linear band structure<br>(Dirac spectrum for mass less fermions) | Field effect transistors                                     | [5]     |
| • High electrical conductivity                                     | Transparent conductive film                                  | [23]    |
| • High-speed electron mobility                                     |  |         |
| • High optical transmittance                                       |  |         |
| • High theoretical surface area                                    | Clean energy devices   | [23]    |
| • Electron transfer along 2d surface                               |  |         |
| • Anomalous quantum hall effect                                    | Ballistic transistors  | [24]    |
| • Irrelevant spin-orbit coupling                                   | Spin-Valve Devices   | [22]    |
| • High conductivity  | Conductive materials, electrical batteries, super capacitors | [2]     |
| • Easy absorption of gases   | Contamination control  | [22]    |
| • Transparency (>99%)  | Displays, touch screens                                      | [25]    |
| • High electronic conductivity                                     |  |         |
| • Impermeability   | Coatings   | [26]    |
| • High mechanical stress (hardness)                                | Construction   | [3]     |

**Table 1.** Graphene properties and applications.

## 1.3. Graphene synthesis

Two different routes can be followed to synthesize graphene: **Bottom Up** and **Top Down** (**Figure 3**). *Bottom-Up* route comprised those methods, which use a carbonaceous gas source to produce graphene. The most relevant ones are *epitaxial growth on Silicon Carbide (SiC)* [27] and *chemical vapor deposition (CVD)* [3]. *Top-Down* route is based on the attack of graphite (used as raw material) to break its layers forming graphene sheets [28]. Methods such as

*micromechanical cleavage* [5, 22], *exfoliation of graphite intercalation compounds (GICs)* [29], *arc discharge* [30, 31], *unzipping carbon nanotubes (CNTs)* [32, 33], *graphene oxide exfoliation* [27] and *solvent-base exfoliation* [34–37] comprise the *Top-Down* route.

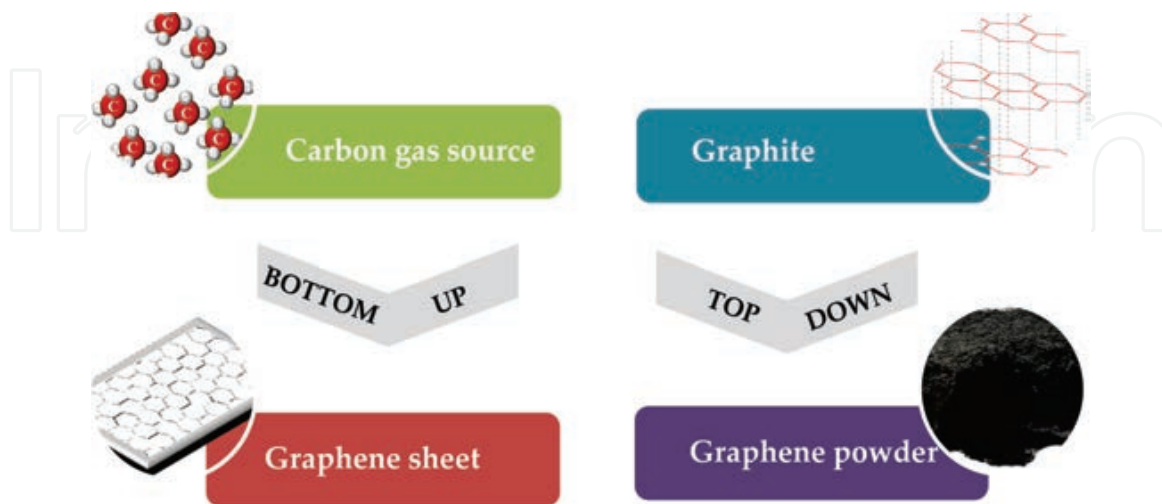


**Figure 3.** *Bottom-Up* and *Top-Down* routes to synthesize graphene.

Among the different *Bottom-Up* synthesis methods, *CVD* is considered the most extensively one used to synthesize large amounts of high-quality graphene sheets. This method is simple and easily scalable [38]. It is important to highlight that the quality and the type of graphene (monolayer, bilayer, few layer, or multilayer) can be varied as a function of the catalytic metal used [3, 39, 40].

On the other hand, the simultaneous reduction and exfoliation of graphene oxide can be considered, among the different *Top-Down* synthesis methods, the easiest one to synthesize graphene-based powder materials. However, the synthesis of graphite oxide (GrO) is first required since it is the intermediate product leading to graphene oxide from graphite. Graphite oxide synthesis is an exothermic process that involves the use of strong acid solutions. In addition, it can be considered as a tedious procedure because many steps are required before the ultimate product is obtained.

Next, the most relevant results obtained in the *CVD* synthesis of graphene are summarized using nickel and copper as catalytic metals, with particular emphasis on the optimization of the main operating variables (synthesis time, temperature, and amount of gases involved during the synthesis). Similarly, the synthesis of graphite oxide is also described. In the latter case, the optimization study here reported pursued the reduction of the time of preparation and the amount of chemical oxidants used during the synthesis of this intermediate product.

## 2. Chemical vapor deposition of graphene layers

Chemical vapor deposition (*CVD*) is a *Bottom-Up* technique, which allows to synthesize wafer-scale graphene [41, 42]. In the *CVD* procedure, a metal substrate, which is used as the catalyst,

is placed into a furnace and heated to high temperatures. The heat anneals the metal, increasing its domain size [43]. Nitrogen, a carbon source (such as methane), and hydrogen are flowed through the furnace during the graphene synthesis. Hydrogen catalyzes the reaction produced between the carbon source and the metal substrate resulting in carbon atoms coming from the carbon source decomposition, which are deposited onto the metal surface through chemical absorption [3]. Hydrogen activates the carbon bonds of the metal surface and controls the size and morphology of graphene domains [44]. After the reaction, the furnace is cooled to keep the deposited carbon atom layer from aggregating into bulk graphite, which crystallizes into a contiguous graphene layer on the metal surface [45]. This method has the advantage of producing large size and high-quality graphene layers, and the ability to synthesize graphene at wafer scale [41]. Moreover, it is considered a low-cost method leading to a high yield if compared to other growth methods. However, the CVD graphene tends to wrinkle due to the difference in thermal expansion between graphene and metal layer. This fact could be decreased via proper annealing [43]. Nickel and copper are commonly used in the CVD method as the metal substrate material for graphene synthesis [46]. Other transition metals such as Ru, Co, and Pt are alternative transition metals, although they are used less frequently [47, 48].

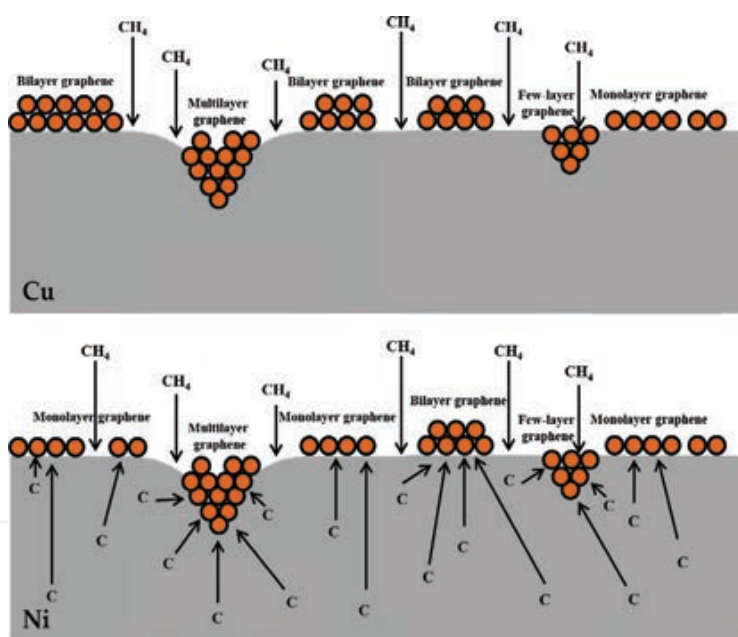


Figure 4. CVD growth-mechanism graphene on copper and nickel sheets [50].

Depending on the metal used, two different mechanisms can be differentiated in the CVD-graphene synthesis (Figure 4). The first one, called *Carbon atoms surface deposition*, which is the growth mechanism observed over copper sheets, is described like the direct deposition of carbon atoms on the catalyst surface. In the second one, called *Carbon atoms surface segregation*, which is the growth mechanism observed when nickel is used as the catalyst, carbon atoms decomposed from the carbonaceous source are diffused onto the catalyst bulk during the annealing step at high temperatures. Then, they precipitate on the catalyst during the cooling period [49].



## 2.1. Optimization of the CVD operational parameters

Several studies have established a close correlation between the *CVD* growth parameters, the quality of the graphene obtained, and the number of graphene layers, leading to the formation of different types of graphene (named as monolayer, bilayer, few layer, and multilayer) on the metal substrate [51–55].

Zhang et al. [51] and Nie et al. [52] found that the graphene quality improved at higher temperatures of reaction. On the contrary, lower temperatures gave rise to graphene with a number of defects. Rybin et al. reported that the larger the temperature of reaction, the higher the amount of atoms dissolved into the metal layer, leading to the production of more and more graphene layers [53].

Recent studies have showed that the concentration of hydrogen, which is obviously related with the  $\text{CH}_4/\text{H}_2$  flow rate ratio and the total flow rate of  $\text{CH}_4$  and  $\text{H}_2$  during the reaction step, also plays an important role in providing quality to *CVD* graphene. Gao et al. found for an atmospheric pressure *CVD* system that high hydrogen concentrations contributes to the degradation of the graphene quality as a result of the occurrence of defects and wrinkles [54]. In a similar way, Vlassioux et al. detected the presence of a critical value of the partial hydrogen that determines the occurrence of graphene growth (<2 Torr with 30 ppm of  $\text{CH}_4$ ). No graphene nucleation was observed below this value, whereas higher hydrogen concentrations caused degradation in graphene quality [44]. Finally, several groups have shown that the growth of bilayer and few-layer graphene depends on the concentration of active carbon species [55], which was in turn related with the  $\text{CH}_4/\text{H}_2$  flow ratio and the total flow rate of  $\text{CH}_4$  and  $\text{H}_2$  used during the reaction step.

On the other hand, monocrystalline metals favor the formation of superficial and uniform monolayer, and bilayer graphene, being hindered the formation of multilayer graphene due to graphene, is grown over smooth and free defect surfaces (**Figure 4**). However, the industrial production of graphene strongly recommends to use polycrystalline metals, since it is much lower than that of monocrystalline one [56].

**Figure 5a** shows the experimental installation used for *CVD*-graphene synthesis over polycrystalline metals (Ni and Cu). **Figure 5b** shows the stages followed during the graphene synthesis as well the duration, temperature, and gases used in each of them.

Methane and hydrogen were actually used as precursor gases. Graphene samples were grown by *CVD* at atmospheric pressure on 25- $\mu\text{m}$ -thick polycrystalline metal foils in a 40-inch quartz tube heated in a furnace. Firstly, the reduction step was carried out by heating the furnace to 900°C, passing through the tube a flow of  $\text{N}_2$  (400 sccm) and  $\text{H}_2$  (100 sccm) to prevent metal sheet oxidation. The annealing step was carried out by maintaining the furnace at this temperature for 45 min. Later, the reaction step was started and carried out at different operational conditions in order to improve the quality of the obtained graphene by decreasing the amount of multilayer graphene formed over the metal. The temperature set point was increased and varied in the range of 900–1050°C. A ratio of methane to hydrogen in the range 0.4–0.07 v/v was introduced into the reactor for different times (15 min to 30 s) to complete the

reaction step. The total flow of gases involved during the reaction step ranged from 80 to 100 Nml/min. Finally, the system was cooled down ( $10^{\circ}\text{C min}^{-1}$ ) by flowing 400 sccm of nitrogen.

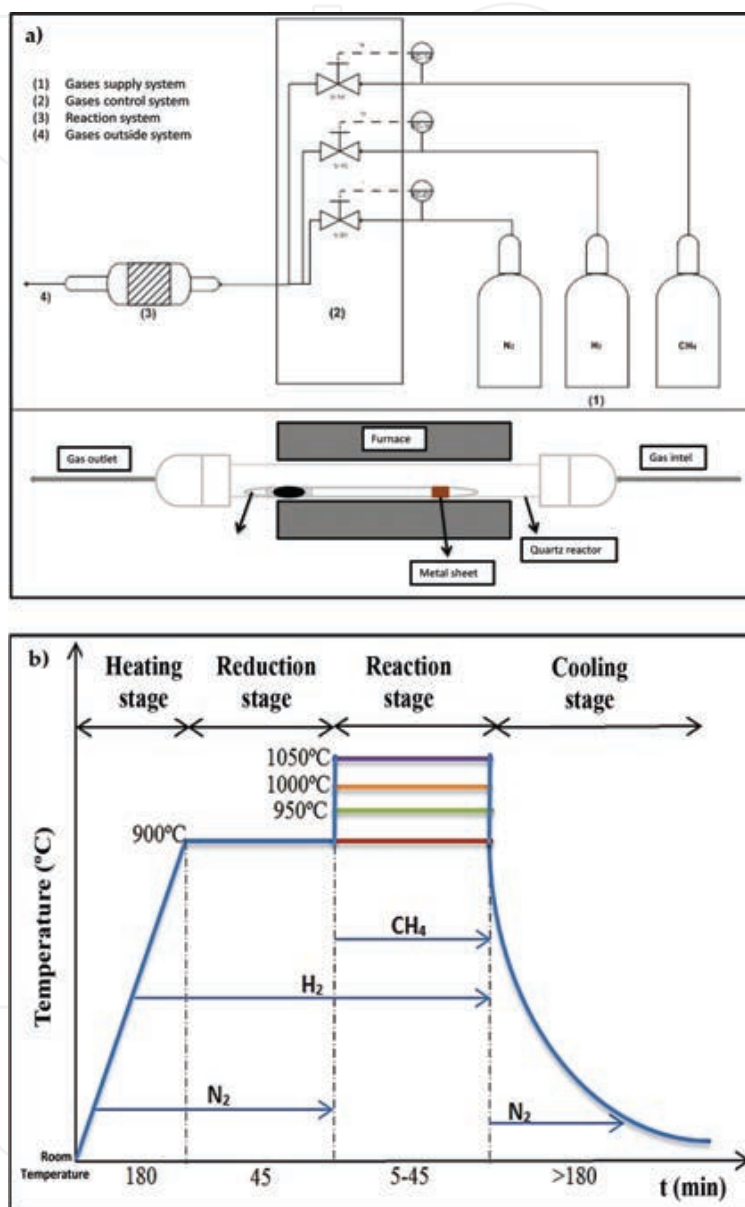


**Figure 5.** (a) Experimental installation for CVD graphene synthesis. (b) Summary of the CVD-graphene synthesis steps and conditions.

To control the graphene thickness and determine the percentage of each type of graphene (monolayer, bilayer, few layer, and multilayer) deposited over the polycrystalline metal foils, a homemade Excel-VBA application was designed. This software used the different colors present in a digitalized optical microscope image to evaluate the percentage of the different types of graphene deposited over the metal sheets. By using Raman spectroscopy, the



relationship between the different colors present in optical images has been demonstrated with each type of graphene [3]. For this purpose, a logarithmic scale was considered in the Excel-VBA software design. Thus, *thickness values* 1, 10, 100, and 1000 were assigned when the 100% of the sample was covered by multilayer, few-layer, bilayer, and monolayer graphene, respectively. The *thickness value* was calculated as an average of the percentage obtained for each type of graphene calculated by the Excel-VBA application.

Ferrari et al. [57] demonstrated that using the second-order 2D feature obtained in the Raman spectra, it was possible to know the number of graphene layers. Based on that study, Malard et al. [58] investigated the theoretical background associated with the double-resonance Raman-scattering mechanism that gives rise to the main feature in the Raman spectra of the different types of graphene. Thus, the deconvolution of the 2D peak, corresponding to each type of graphene, showed that in the case of monolayer graphene the 2D peak could be fitted with a symmetric single peak only; in the case of bilayer graphene, the 2D peak could be deconvoluted in four different contributions; in the case of few-layer and multilayer graphene, the 2D peak could be deconvoluted in two contributions, which is characteristic of graphite (material consisting of many layers of graphene) (**Figure 6**).

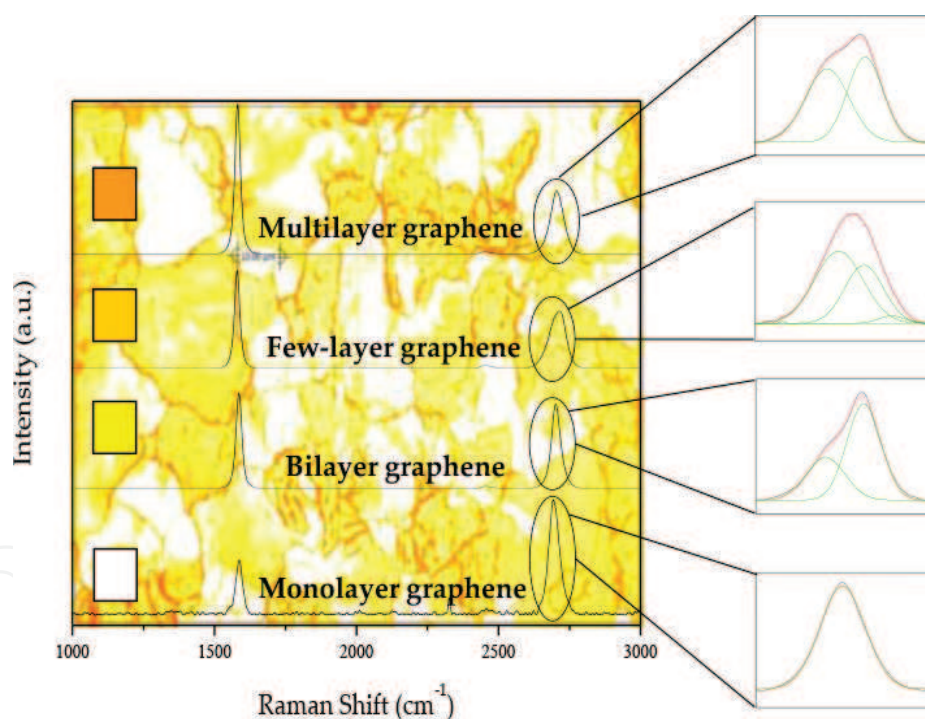


**Figure 6.** Relationship between optical microscope image and typical Raman spectra of monolayer [48, 59–61], bilayer [47, 59, 60, 62], few layer [63–65], and multilayer [63, 64] graphene.

In this study, polycrystalline copper and nickel were chosen as metal catalyst in the synthesis of CVD graphene.

Regarding polycrystalline Cu, 1050°C was required to maximize the amount of monolayer graphene over the metal, whereas 980°C was selected as the optimum reaction temperature in the case of using polycrystalline nickel. In the former case, the *thickness value* was found to be

4.2, the proportion of each type of graphene being the following one: 81% multilayer graphene, 17% few-layer graphene, and 2% bilayer graphene; the presence of monolayer graphene was considered negligible. In the latter case, the *thickness value* was found to be 397, in turn the proportion of each type of graphene being the following one: 0.9% multilayer graphene, 40% few-layer graphene, 22% bilayer graphene, and 37% monolayer graphene.

Regarding the CH<sub>4</sub>/H<sub>2</sub> flow rate ratio, an optimal value of 0.07 v/v was obtained when both metals were used as catalysts. A *thickness value* of 34.7 was obtained using Cu (20% multilayer graphene, 20% few-layer graphene, and 51% bilayer graphene), whereas a *thickness value* of 536 was obtained using Ni (0.5% multilayer graphene, 27% few-layer graphene, 20% bilayer graphene, and 52% monolayer graphene).

Finally, regarding the study of the influence of the total flow of gases (CH<sub>4</sub>+ H<sub>2</sub>) and reaction time, it could be concluded that the best results in the case of using Cu as the catalyst were obtained for a total gas flow of 60 Nml/min and a reaction time of 10 min, leading to an increased *thickness value* of 60, 56 and 11% of the resulting sample being covered by bilayer graphene and multilayer graphene, respectively. In the case of using Ni as the catalyst, the best results were obtained for a total gas flow of 80 Nml/min and a reaction time of 1 min (*thickness value* of 810). At these conditions, just 0.3% of the sample was covered by multilayer graphene, 11% by few-layer graphene, 9% by bilayer graphene, and 80% by monolayer graphene.

| Variable   | Copper | Nickel |
|--|--------|--------|
| Reaction temperature (°C)  | 1050   | 980    |
| CH <sub>4</sub> /H <sub>2</sub> flow rate ratio (v/v)                  | 0.07   | 0.07   |
| Total gas flow (CH <sub>4</sub> +H <sub>2</sub> ) during reaction step | 60     | 80     |
| Reaction time (min)  | 10     | 1      |
| Graphene type  |        |        |
| <i>Thickness value</i>   | 59     | 810    |

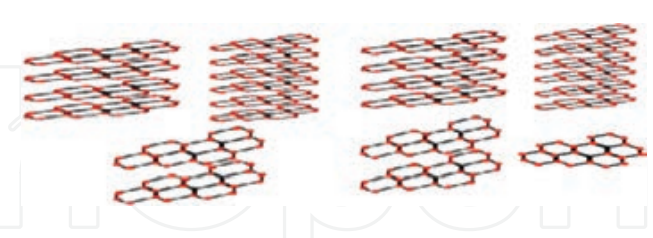


**Table 2.** Optimum synthesis conditions.

Summarizing, the *thickness value* was increasing at each stage of the optimization study regardless of the metal used. However, it was not possible to detect monolayer graphene on polycrystalline copper foil. In the case of using polycrystalline nickel, monolayer graphene covered 80% of the foil for the optimal conditions of synthesis.

**Table 2** shows the optimum operating conditions for each metal resulting from this study.

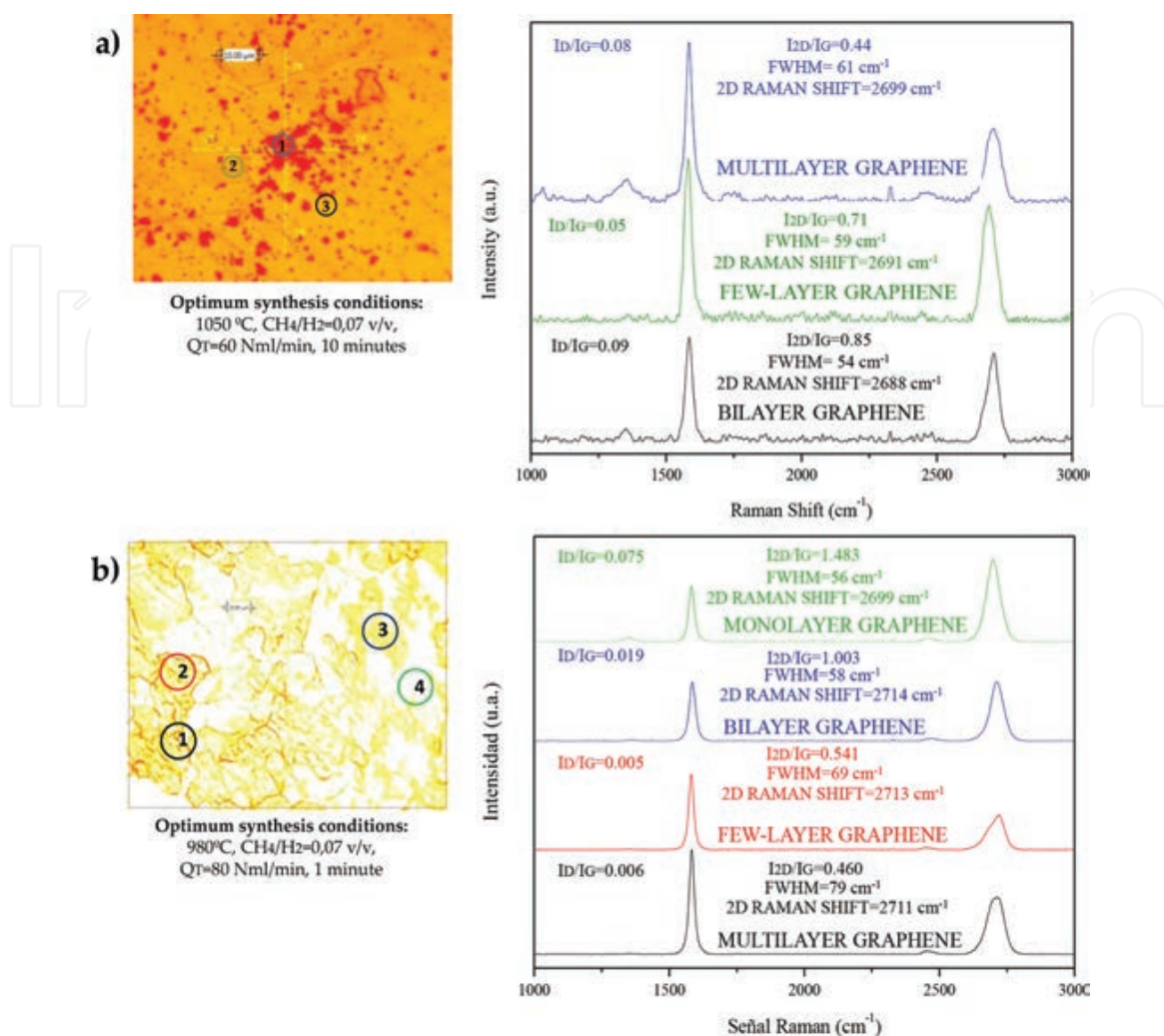


**Figure 7.** Raman spectra corresponding to graphene samples synthesized using (a) copper and (b) nickel.

**Figure 7** shows the Raman spectra corresponding to the graphene samples obtained at the optimal conditions. D peak ( $1350\text{ cm}^{-1}$ ) is related to the presence of defects in graphitic materials [66]. G peak ( $\sim 1560\text{ cm}^{-1}$ ) denotes the symmetry of graphite band and is a way of checking the vibration of  $\text{sp}^2$ -hybridized carbon atoms in the same plane. Finally, 2D peak, visible around  $2700\text{ cm}^{-1}$ , is the hallmark of graphene layers [67]. The relationship between the intensity of D and G peak ( $I_D/I_G$ ) is a way to check the amount of defects present in the graphene sheet. The number of graphene layer is also related to the ratio between the intensity of 2D and G peak ( $I_{2D}/I_G$ ). 2D peak position in graphene sample should be displaced to lower Raman shift values in comparison with that of graphite. Finally, full width at half maximum (FWHM) is related to the lifetime of the excited states and is calculated as the Raman shift difference to the half average height of the 2D peak [39]. For both metal catalysts, the  $I_D/I_G$  ratio values were low, demonstrating that graphene samples had low amount of defects, whereas the  $I_{2D}/I_G$  ratio values increased, as expected, from multilayer to monolayer graphene [68]. The contrary effect could be observed for the FWHM parameter, which decreased from multilayer to monolayer graphene. Finally, 2D peak position was, in all cases, located at around  $2700\text{ cm}^{-1}$ , which is characteristic of graphene materials [3, 39].

### 3. Graphite oxide

Graphite oxide (GrO) can be defined as a set of functionalized graphene sheets that are mainly composed of carbon, oxygen, and hydrogen atoms. This material is considered a precursor of graphene itself [69]. The structure of graphite oxide is similar to that of graphite differing only in the oxygenated groups present in GrO, which give rise to a greater distance between the graphene layers [69]. GrO consists of a hexagonal network of  $sp^2$ - and  $sp^3$ -hybridized carbon atoms that bear hydroxyl and epoxide functional groups on the 'basal' plane and carboxyl and carbonyl groups at the edges [70].

#### 3.1. Graphite oxide synthesis

Graphite oxide can be synthesized by the Brodie [7], Staudenmaier [8], or Hummers and Offeman [9] methods or by variations of the latter, namely *Modified Hummers method* or *Improved Hummers method* [71]. The main differences between the abovementioned methods are summarized in **Table 3**, with particular emphasis on the nature of the oxidant, the toxicity, and the main advantages or disadvantages of each approach.

#### 3.2. Improved Hummers method

In 1958, Hummers reported the most popular procedure to synthesize graphite oxide, which is based on the oxidization of graphite by using  $KMnO_4$  and  $NaNO_3$  in concentrated  $H_2SO_4$  [9]. However, this method yields  $NO_x$  and is dangerous itself due to the constant explosions, which take place during the synthesis [71]. In 2010, Marcano et al. [71] reported an improved synthesis based on the Hummers method by using graphite flakes as the raw material. Graphite oxide synthesized from graphite flakes can be easily soaked and dispersed in water and could be used as the precursor for different applications due to its hydrophilic character. They detected that an improved graphite oxide with fewer defect in the basal plane can be prepared using  $KMnO_4$  as oxidation agent and a 9:1 mixture of concentrated  $H_2SO_4$  and  $H_3PO_4$ . They also reported that graphite oxide synthesized with this *Improved Hummers method* provided a greater amount of hydrophilic-oxidized graphite, likewise having a more regular structure with a greater amount of basal plane framework retained. Raman and infrared spectroscopy results indicated that graphite oxide samples obtained through both methods were almost similar, both of them showing the characteristics D and G peaks that confirmed the lattice distortion in Raman spectroscopy. FTIR-ATR spectra also confirmed the presence of functional groups. In addition, atomic force microscopy (AFM) showed that the thickness of both graphite oxides was around 1.1 nm. They confirmed with a large variety of methods, such as thermogravimetry analysis (TGA), solid-state colossal magnetoresistance (CMR), X-ray diffraction (XRD), and X-ray photoelectron spectroscopy (XPS), that graphite oxide synthesized with the *Improved Hummers method* was, if it is compared to that produced from the Hummers one, a more oxidized material, presented a more organized structure, and contained both more epoxide functionalities, and more regular carbon framework.



| Brodie Method   | Staudenmaier Method  | Hummers Method  | Modified Hummers Method   | Improved Hummers Method  |
|---|--|---|---|--|
| <p><b>Oxidants:</b><br/>KClO<sub>3</sub>, HNO<sub>3</sub></p> <p><b>Toxicity:</b> Yes</p> <p><b>Disadvantages:</b></p> <ul style="list-style-type: none"> <li>•Weak Toxicity.</li> <li>•Soft dispersability in basic solutions.</li> <li>•Small size, limiting thickness and providing an imperfect structure.</li> </ul> | <p><b>Oxidants:</b><br/>KClO<sub>3</sub>, (NaClO<sub>3</sub>), HNO<sub>3</sub>, H<sub>2</sub>SO<sub>4</sub></p> <p><b>Toxicity:</b> Yes</p> <p><b>Disadvantages:</b></p> <ul style="list-style-type: none"> <li>•Time-consuming and dangerous method.</li> <li>•Addition of KClO<sub>3</sub> generally takes longer than a week and CO<sub>2</sub> is evolved, thus making necessary to remove an inert gas.</li> <li>•The risk of explosions is a constant danger.</li> </ul> | <p><b>Oxidants:</b><br/>KMnO<sub>4</sub>, H<sub>2</sub>SO<sub>4</sub>, NaNO<sub>3</sub></p> <p><b>Toxicity:</b> No (NO<sub>x</sub>)</p> <p><b>Advantages:</b></p> <ul style="list-style-type: none"> <li>•Higher oxidation degree than that obtained in Brodie or Staudenmaier Methods.</li> </ul> <p><b>Disadvantages:</b></p> <ul style="list-style-type: none"> <li>•It is still considered that the oxidation is incomplete.</li> </ul> | <p><b>Oxidants:</b><br/>KMnO<sub>4</sub>, H<sub>2</sub>SO<sub>4</sub>, NaNO<sub>3</sub></p> <p><b>Toxicity:</b> No (NO<sub>x</sub>)</p> <p><b>Advantages:</b></p> <ul style="list-style-type: none"> <li>•Improved level of oxidation and, therefore, product performance.</li> </ul> <p><b>Disadvantages:</b></p> <ul style="list-style-type: none"> <li>•Separation and purification processes are tedious.</li> <li>•Highly time-consuming.</li> </ul> | <p><b>Oxidants:</b><br/>KMnO<sub>4</sub>, H<sub>2</sub>SO<sub>4</sub>, H<sub>3</sub>PO<sub>4</sub></p> <p><b>Toxicity:</b> No</p> <p><b>Advantages:</b></p> <ul style="list-style-type: none"> <li>•Defects in the basal plane are reduced.</li> <li>•Larger amount of oxidized graphite is provided.</li> <li>•The degree of reduction provides an equivalent level of conductivity when compared to other methods.</li> <li>•It is a high performance method.</li> <li>•Environmentally friendly, toxic gases are not generated during the preparation.</li> <li>•The product has a more organized structure.</li> </ul> |

**Table 3.** Synthesis methods of graphite oxide.

### 3.3. Optimization of the Improved Hummers method

The most remarkable results obtained in the optimization study of the synthesis of graphite oxide based on the method proposed by Marcano et al. [71] (*Improved Hummers method*) are summarized below. Thus, the objective was to reach the same quality product but using a lesser time-consuming experimental procedure and conducting lower production costs. With this purpose, the different stages of the *Improved Hummers method* used in the synthesis of graphite oxide were optimized. The method consists of the oxidation, in the presence of H<sub>2</sub>SO<sub>4</sub> and H<sub>3</sub>PO<sub>4</sub>, of 3 g of graphite per 9 g of KMnO<sub>4</sub> used as the oxidizing agent in 400 ml of solution. The oxidation step is maintained at 50°C for 12 h. Later, the reaction mixture is washed twice with 200 ml of deionized water, HCl, and ethanol. Finally, the product is coagulated with 200 ml of dry diethyl ether and dried at 100°C [71].



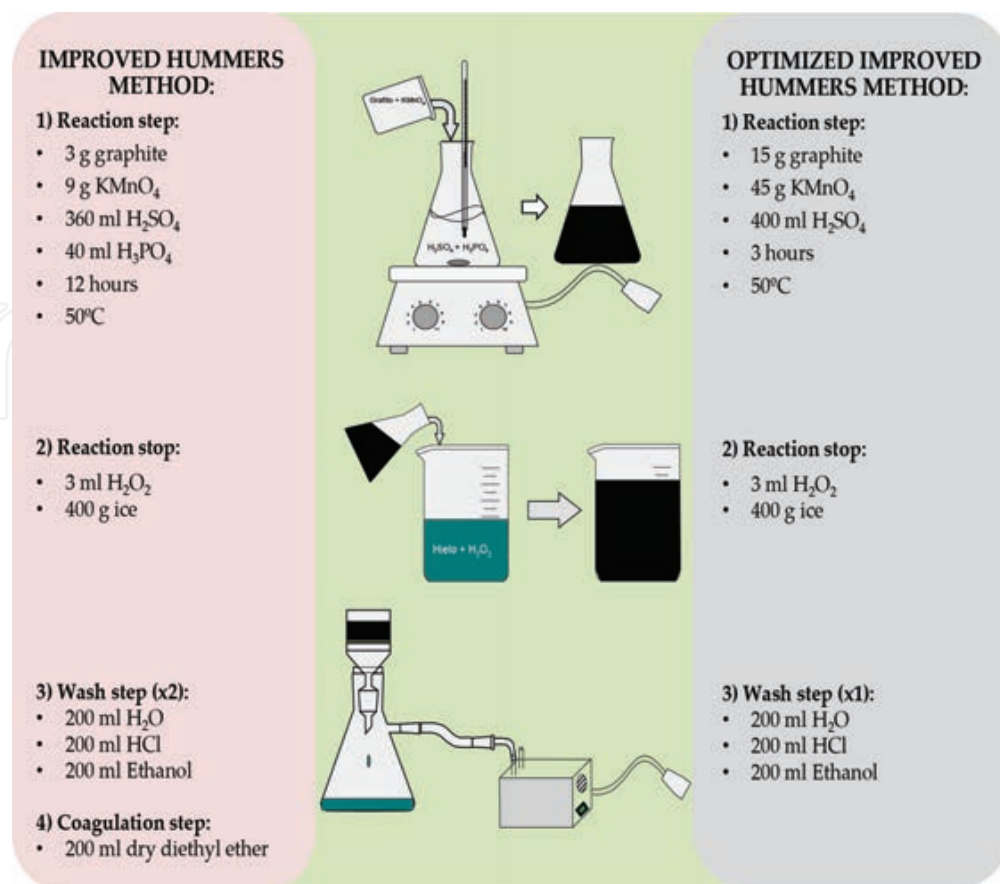


Figure 8. Differences between the *Improved Hummers* and *Optimized Improved Hummers* methods.


First, the oxidation time, which is the most time-consuming step of the whole synthesis process, was reduced. This way, the oxidation time was reduced from 12 to 3 h, whereas the other synthesis conditions were kept constant without affecting the quality of the final product. The introduction of functional groups, both at the edges and in the basal plane, was achieved in 3 h instead of the 12 h required in the original method.

Second, it was demonstrated that the coagulation step used by Marcano et al. [71] did not significantly influence over the quality and characteristic properties of the final product. Consequently, it was removed from the synthesis procedure.

On the other hand, Marcano et al. used three different products twice during the washing step: deionized water, which was used to reach the pH neutralization; HCl, which was required to remove the remaining metal from the graphite oxide, and ethanol, which was used to achieve a faster drying of the final product. We demonstrated that the quality and characteristic of the final product were not affected at all if the treatment of the cake with these three products was or not repeated. In addition, the elimination of  $\text{H}_3\text{PO}_4$  in the synthesis procedure was considered. Similarly, this action did not alter the characteristics of the final product.

Finally, a series of tests were conducted in order to increase the amount of graphite that can be treated per batch, without altering the properties of the final product (the raw method

considers 3 g of graphite and 9 g of  $\text{KMnO}_4$  in 400 ml of solution). Here, the  $\text{KMnO}_4$ /graphite ratio (3:1) was maintained in order to not alter the degree of oxidation. This way, the amount of these materials was progressively increased. It was observed that it was possible to use up to 15 g of graphite (and hence 45 g of  $\text{KMnO}_4$ ) in 400 ml of solution without altering the characteristics and quality of the product. **Figure 8** schematically summarizes the differences between the original method (*Improved Hummers method*) and the optimized one (*Optimized Improved Hummers method*).

|                              | Graphite   | Improved Hummers method | Optimized Improved Hummers method |
|------------------------------|--|-------------------------|-----------------------------------|
| Raman spectroscopy $I_D/I_G$ | 0.067  | 0.726                   | 0.946                             |
|                              | $L_a$ (nm)   | 263                     | 20.4                              |
| <b>DRX</b>                   | $L_a$ (nm)   | 41                      | 10.1                              |
|                              | $L_c$ (nm)   | 20                      | 4.9                               |
|                              | $d_{002}$ (nm)   | 0.334                   | 0.910                             |
|                              | $N_c$  | 60                      | 5.4                               |
| <b>Elemental composition</b> | C  | 98.04                   | 51.4                              |
|                              | O  | 1.96                    | 45.1                              |
|                              | S  | 0.0                     | 2.8                               |
|                              | Cl   | 0                       | 0.6                               |
|                              | Mn   | 0                       | 0.1                               |
| <b>SEM</b>                   |  |                         |                                   |
| <b>BET</b>                   | Surface area ( $\text{m}^2/\text{g}$ )   | 1.7                     | 22.2                              |
|                              | Total pore volume ( $\text{cm}^3/\text{g}$ )   | 0.038                   | 0.113                             |

**La:** crystal dimension described by layer sized; **Lc:** stack height; **Nc:** number of layers in the stacking structure; **C:** carbon, **O:** oxygen, **S:** sulfur, **Cl:** chlorine; **Mn:** manganese.

**Table 4.** Characterization results of graphite oxide synthesized using both the *Improved Hummers* and *Optimized Improved Hummers methods*.

**Table 4** lists some properties of the graphite oxide samples synthesized by the *Optimized Improved Hummers method* and those prepared from the parent one.  $I_D/I_G$  ratio, related with the structural disorder in the graphite network and inversely proportional to the  $\text{sp}^2$  cluster average sized [72], considerably increased after graphite oxidation. Crystal dimension ( $L_a$  value) decreased after the incorporation of oxygenated groups, which agree with the increase in the structural disorder. In the same way, the number of graphene layers in the stacking

structure ( $N_c$ ) decreased after the oxidation process [73]. Elemental analysis showed an increase in the percentage of oxygen from graphite to graphite oxide due to the oxidation process. Comparing both graphite oxides, the percentage of each compound (C, O, S, Cl, and Mn) was quite similar [74]. In addition, scanning electron microscope (SEM) images showed an agglomeration of the product after the oxidation process, being several microns in size. Finally, a significant increase in the surface area was observed after graphite oxidation, because of the expansion of graphene layers [75].

The almost similar characterization values of both samples of graphite oxide demonstrated that the optimization process did not affect both quality and structure of the final product.

## Acknowledgements

The present work was performed within the frame of the NANOLEAP project. This project has received funding from the European Union's Horizon 2020 research and innovation programme under grant agreement No 646397.

## Author details

María del Prado Lavín López\*, José Luis Valverde Palomino, María Luz Sánchez Silva and Amaya Romero Izquierdo

\*Address all correspondence to: [MariadelPrado.Lavin@uclm.es](mailto:MariadelPrado.Lavin@uclm.es)

Department of Chemical Engineering, University of Castilla-La Mancha, Ciudad Real, Spain

## References

- [1] Adler J, Pine P. Visualization techniques for modelling carbon allotropes. *Computer Physics Communications*. 2009;180:580–582. DOI: 10.1016/j.cpc.2008.12.014.
- [2] Geim AK, Novoselov KS. The rise of graphene. *Nature Materials*. 2007;6:183–191. DOI: 10.1038/nmat1849.
- [3] Lavin-Lopez MP, Valverde JL, Cuevas MC, Garrido A, Sanchez-Silva L, Martinez P, Romero-Izquierdo A. Synthesis and characterization of graphene: Influence of synthesis variables. *Physical Chemistry Chemical Physics*. 2014;16:2962–2970. DOI: 10.1039/c3cp54832e.

- [4] Horing NJM. Aspects of the theory of graphene. *Philosophical Transactions of the Royal Society A: Mathematical, Physical and Engineering Sciences*. 2010;368:5525–5556. DOI: 10.1098/rsta.2010.0242.
- [5] Novoselov KS, Geim AK, Morozov SV, Jiang D, Zhang Y, Dubonos SV, Grigorieva IV, Firsov AA. Electric field in atomically thin carbon films. *Science*. 2004;306:666–669. DOI: 10.1126/science.1102896.
- [6] Lavin-Lopez MP, Valverde JL, Sanchez-Silva, L, and Romero A. Solvent-based exfoliation via sonication of graphitic materials for graphene manufacture. *Industrial & Engineering Chemistry Research*. 2016;55:845–855. DOI: 10.1021/acs.iecr.5b03502.
- [7] Brodie BC. XXIII. – Researches on the atomic weight of graphite. *Quarterly Journal of the Chemical Society of London*. 1860;12:261–268. DOI: 10.1039/qj8601200261.
- [8] Staudenmaier L. A process for the presentation of graphite acid. *Reports of the German Chemical Society*. 1898;31:1481–1487.
- [9] Hummers Jr WS, Offeman RE. Preparation of graphitic oxide. *Journal of the American Chemical Society*. 1958;80:1339.
- [10] Boehm HP, Clauss A, Fischer GO, Hofmann U. Thinnest carbon foils. *Journal for Nature Research – Section B*. 1962;17:150–153. DOI: 10.1515/znb-1962-0302.
- [11] Morgan AE, Somorjai GA. Low energy electron diffraction studies of gas adsorption on the platinum (100) single crystal surface. *Surface Science*. 1968;12:405–425.
- [12] May JW. Platinum surface LEED rings. *Surface Science*. 1969;17:267–270.
- [13] Blakely JM, Kim JS, Potter HC. Segregation of carbon to the (100) surface of nickel. *Journal of Applied Physics*. 1970;41:2693–2697. DOI: 10.1063/1.1659283.
- [14] Van Bommel AJ, Crombeen JE, Van Tooren A. LEED and Auger electron observations of the SiC(0001) surface. *Surface Science*. 1975;48:463–472. DOI: 10.1016/0039-6028(75)90419-7.
- [15] Boehm HP, Setton R, Stumpp E. Nomenclature and terminology of graphite intercalation compounds. *Carbon*. 1986;24:241–245. DOI: 10.1016/0008-6223(86)90126-0.
- [16] IUPAC - International Union of Pure and Applied Chemistry: Home [Internet]. 1997. Available from: <http://goldbook.iupac.org/G02683.html>. [Accessed: 2016 01-23].
- [17] Lu X, Yu M, Huang H, Ruoff RS. Tailoring graphite with the goal of achieving single sheets. *Proceedings of the 1998 6th Foresight Conference on Molecular Nanotechnology*. 1999;10:269–272. DOI: 10.1088/0957-4484/10/3/308.
- [18] Novoselov KS, Geim AK, Morozov SV, Jiang D, Katsnelson MI, Grigorieva IV, Dubonos SV, Firsov AA. Two-dimensional gas of massless Dirac fermions in graphene. *Nature*. 2005;438:197–200. DOI: 10.1038/nature04233.

- [19] N'Diaye AT, Bleikamp S, Feibelman PJ, Michely T. Two-dimensional Ir cluster lattice on a graphene moiré on Ir(111). *Physical Review Letters*. 2006;97. DOI: 10.1103/PhysRevLett.97.215501.
- [20] Kungliga Vetenskapsakademien – Hem [Internet]. 2010. Available from: <http://www.kva.se/en/> [Accessed: 2016 01-23].
- [21] Graphene Flagship [Internet]. 2013. Available from: <http://graphene-flagship.eu/> [Accessed: 2016 01-24].
- [22] Katsnelson MI. Graphene: carbon in two dimensions. *Materials Today*. 2007;10:20–27. DOI: 10.1016/s1369-7021(06)71788-6.
- [23] Zhu Y, Murali S, Cai W, Li X, Suk JW, Potts JR, Ruoff RS. Graphene and graphene oxide: synthesis, properties, and applications. *Advanced Materials*. 2010;22:3906–3924. DOI: 10.1002/adma.201001068.
- [24] Geim AK, Dubonos SV, Lok JGS, Grigorieva IV, Maan JC, Theil Hansen L, Lindelof PE. Ballistic hall micromagnetometry. *Applied Physics Letters*. 1997;71:2379–2381.
- [25] Nair RR, Wu HA, Jayaram PN, Grigorieva IV, Geim AK. Unimpeded permeation of water through helium-leak-tight graphene-based membranes. *Science*. 2012;335:442–444. DOI: 10.1126/science.1211694.
- [26] Boukhvalov DW, Katsnelson MI. Chemical functionalization of graphene. *Journal of Physics Condensed Matter*. 2009;21. DOI: 10.1088/0953-8984/21/34/344205.
- [27] Whitener Jr KE, Sheehan PE. Graphene synthesis. *Diamond and Related Materials*. 2014;46:25–34. DOI: 10.1016/j.diamond.2014.04.006.
- [28] Edwards RS, Coleman KS. Graphene synthesis: relationship to applications. *Nanoscale*. 2013;5:38–51. DOI: 10.1039/c2nr32629a.
- [29] Vallés C, Drummond C, Saadaoui H, Furtado CA, He M, Roubeau O, Ortolani L, Monthieux M, Pénicaud A. Solutions of negatively charged graphene sheets and ribbons. *Journal of the American Chemical Society*. 2008;130:15802–15804. DOI: 10.1021/ja808001a.
- [30] Subrahmanyam KS, Panchakarla LS, Govindaraj A, Rao CNR. Simple method of preparing graphene flakes by an arc-discharge method. *Journal of Physical Chemistry C*. 2009;113:4257–4259. DOI: 10.1021/jp900791y.
- [31] Chen Y, Zhao H, Sheng L, Yu L, An K, Xu J, Ando Y, Zhao X. Mass-production of highly-crystalline few-layer graphene sheets by arc discharge in various H<sub>2</sub>-inert gas mixtures. *Chemical Physics Letters*. 2012;538:72–76. DOI: 10.1016/j.cplett.2012.04.020.
- [32] Jiao L, Zhang L, Wang X, Diankov G, Dai H. Narrow graphene nanoribbons from carbon nanotubes. *Nature*. 2009;458:877–880. DOI: 10.1038/nature07919.



- [33] Valentini L. Formation of unzipped carbon nanotubes by CF<sub>4</sub> plasma treatment. *Diamond and Related Materials*. 2011;20:445–448. DOI: 10.1016/j.diamond.2011.01.038.
- [34] Yi M, Shen Z. A review on mechanical exfoliation for the scalable production of graphene. *Journal of Materials Chemistry A*. 2015;3:11700–11715. DOI: 10.1039/c5ta00252d.
- [35] Blake P, Brimicombe PD, Nair RR, Booth TJ, Jiang D, Schedin F, Ponomarenko LA, Morozov SV, Gleeson HF, Hill EW, Geim AK, Novoselov KS. Graphene-based liquid crystal device. *Nano Letters*. 2008;8:1704–1708. DOI: 10.1021/nl080649i.
- [36] Hernandez Y, Nicolosi V, Lotya M, Blighe FM, Sun Z, De S, McGovern IT, Holland B, Byrne M, Gun'ko YK, Boland JJ, Niraj P, Duesberg G, Krishnamurthy S, Goodhue R, Hutchison J, Scardaci V, Ferrari AC, Coleman JN. High-yield production of graphene by liquid-phase exfoliation of graphite. *Nature Nanotechnology*. 2008;3:563–568. DOI: 10.1038/nnano.2008.215.
- [37] Ciesielski A, Samorì P. Graphene via sonication assisted liquid-phase exfoliation. *Chemical Society Reviews*. 2014;43:381–398. DOI: 10.1039/c3cs60217f.
- [38] Bhuyan SA, Uddin N, Islam M, Bipasha FA, Hossain SS. Synthesis of graphene. *International Nano Letters*. 2016. DOI: 10.1007/s40089-015-0176-1.
- [39] Lavin-Lopez MP, Valverde JL, Ruiz-Enrique MI, Sanchez-Silva L, Romero A. Thickness control of graphene deposited over polycrystalline nickel. *New Journal of Chemistry*. 2015;39:4414–4423. DOI: 10.1039/c5nj00073d.
- [40] Muñoz R, Gómez-Aleixandre C. Review of CVD synthesis of graphene. *Chemical Vapor Deposition*. 2013;19:297–322. DOI: 10.1002/cvde.201300051.
- [41] Obraztsov AN. Chemical vapour deposition: making graphene on a large scale. *Nature Nanotechnology*. 2009;4:212–213. DOI: 10.1038/nnano.2009.67.
- [42] Emtsev KV, Bostwick A, Horn K, Jobst J, Kellogg GL, Ley L, McChesney JL, Ohta T, Reshanov SA, Röhrl J, Rotenberg E, Schmid AK, Waldmann D, Weber HB, Seyller T. Towards wafer-size graphene layers by atmospheric pressure graphitization of silicon carbide. *Nature Materials*. 2009;8:203–207. DOI: 10.1038/nmat2382.
- [43] Bae S, Kim H, Lee Y, Xu X, Park JS, Zheng Y, Balakrishnan J, Lei T, Ri Kim H, Song YI, Kim YJ, Kim KS, Özyilmaz B, Ahn JH, Hong BH, Iijima S. Roll-to-roll production of 30-inch graphene films for transparent electrodes. *Nature Nanotechnology*. 2010;5:574–578. DOI: 10.1038/nnano.2010.132.
- [44] Vlassiuk I, Regmi M, Fulvio P, Dai S, Datskos P, Eres G, Smirnov S. Role of hydrogen in chemical vapor deposition growth of large single-crystal graphene. *ACS Nano*. 2011;5:6069–6076. DOI: 10.1021/nn201978y.

- [45] Kim KS, Zhao Y, Jang H, Lee SY, Kim JM, Ahn JH, Kim P, Choi JY, Hong BH. Large-scale pattern growth of graphene films for stretchable transparent electrodes. *Nature*. 2009;457:706–710.
- [46] López GA, Mittemeijer EJ. The solubility of C in solid Cu. *Scripta Materialia*. 2004;51:1–5. DOI: 10.1016/j.scriptamat.2004.03.028.
- [47] Ruan G, Sun Z, Peng Z, Tour JM. Growth of graphene from food, insects, and waste. *ACS Nano*. 2011;5:7601–7607. DOI: 10.1021/nn202625c.
- [48] Sun Z, Yan Z, Yao J, Beitler E, Zhu Y, Tour JM. Growth of graphene from solid carbon sources. *Nature*. 2010;468:549–552. DOI: 10.1038/nature09579.
- [49] Seah CM, Chai SP, Mohamed AR. Mechanisms of graphene growth by chemical vapour deposition on transition metals. *Carbon*. 2014;70:1–21. DOI: 10.1016/j.carbon.2013.12.073.
- [50] Zhang Y, Zhang L, Zhou C. Review of chemical vapor deposition of graphene and related applications. *Accounts of Chemical Research*. 2013;46:2329–2339. DOI: 10.1021/ar300203n.
- [51] Zhang Y, Gao T, Gao Y, Xie S, Ji Q, Yan K, Peng H, Liu Z. Defect-like structures of graphene on copper foils for strain relief investigated by high-resolution scanning tunneling microscopy. *ACS Nano*. 2011;5:4014–4022. DOI: 10.1021/nn200573v.
- [52] Nie S, Wofford JM, Bartelt NC, Dubon OD, McCarty KF. Origin of the mosaicity in graphene grown on Cu(111). *Physical Review B – Condensed Matter and Materials Physics*. 2011;84. DOI: 10.1103/PhysRevB.84.155425.
- [53] Rybin MG, Pozharov AS, Obraztsova ED. Control of number of graphene layers grown by chemical vapor deposition. *Physica Status Solidi (C) Current Topics in Solid State Physics*. 2010;7:2785–2788. DOI: 10.1002/pssc.201000241.
- [54] Gao L, Ren W, Zhao J, Ma LP, Chen Z, Cheng HM. Efficient growth of high-quality graphene films on Cu foils by ambient pressure chemical vapor deposition. *Applied Physics Letters*. 2010;97. DOI: 10.1063/1.3512865.
- [55] Ma L, Ren W, Dong Z, Liu L, Cheng H. Progress of graphene growth on copper by chemical vapor deposition: growth behavior and controlled synthesis. *Chinese Science Bulletin*. 2012;57:2995–2999. DOI: 10.1007/s11434-012-5335-4.
- [56] Zhang Y, Gomez L, Ishikawa FN, Madaria A, Ryu K, Wang C, Badmaev A, Zhou C. Comparison of graphene growth on single-crystalline and polycrystalline Ni by chemical vapor deposition. *Journal of Physical Chemistry Letters*. 2010;1:3101–3107. DOI: 10.1021/jz1011466.
- [57] Ferrari AC, Meyer JC, Scardaci V, Casiraghi C, Lazzeri M, Mauri F, Piscanec S, Jiang D, Novoselov KS, Roth S, Geim AK. Raman spectrum of graphene and graphene layers. *Physical Review Letters*. 2006;97. DOI: 10.1103/PhysRevLett.97.187401.

- [58] Malard LM, Pimenta MA, Dresselhaus G, Dresselhaus MS. Raman spectroscopy in graphene. *Physics Reports*. 2009;473:51–87. DOI: 10.1016/j.physrep.2009.02.003.
- [59] Wang YY, Ni ZH, Yu T, Shen ZX, Wang HM, Wu YH, Chen W, Wee ATS. Raman studies of monolayer graphene: the substrate effect. *Journal of Physical Chemistry C*. 2008;112:10637–10640. DOI: 10.1021/jp8008404.
- [60] Rümeli MH, Rocha CG, Ortman F, Ibrahim I, Sevincli H, Börrnert F, Kunstmann J, Bachmatiuk A, Pötschke M, Shiraishi M, Meyyappan M, Büchner B, Roche S, Cuniberti G. Graphene: piecing it together. *Advanced Materials*. 2011;23:4471–4490. DOI: 10.1002/adma.201101855.
- [61] Gong Y, Zhang X, Liu G, Wu L, Geng X, Long M, Cao X, Guo Y, Li W, Xu J, Sun M, Lu L, Liu L. Layer-controlled and wafer-scale synthesis of uniform and high-quality graphene films on a polycrystalline nickel catalyst. *Advanced Functional Materials*. 2012;22:3153–3159. DOI: 10.1002/adfm.201200388.
- [62] Chen S, Cai W, Piner RD, Suk JW, Wu Y, Ren Y, Kang J, Ruoff RS. Synthesis and characterization of large-area graphene and graphite films on commercial Cu-Ni alloy foils. *Nano Letters*. 2011;11:3519–3525. DOI: 10.1021/nl201699j.
- [63] Dahal A, Batzill M. Graphene-nickel interfaces: a review. *Nanoscale*. 2014;6:2548–2562. DOI: 10.1039/c3nr05279f.
- [64] Calizo I, Teweldebrhan D, Bao W, Miao F, Lau CN, Balandin AA. Spectroscopic Raman nanometrology of graphene and graphene multilayers on arbitrary substrates. *Journal of Physics: Conference Series*. 2008;109:5. DOI: 10.1088/1742-6596/109/1/012008.
- [65] Das A, Chakraborty B, Sood AK. Raman spectroscopy of graphene on different substrates and influence of defects. *Bulletin of Materials Science*. 2008;31:579–584. DOI: 10.1007/s12034-008-0090-5.
- [66] Wall M. Raman spectroscopy optimizes graphene characterization. *Advanced Materials and Processes*. 2012;170:35–38.
- [67] Suk JW, Kitt A, Magnuson CW, Hao Y, Ahmed S, An J, Swan AK, Goldberg BB, Ruoff RS. Transfer of CVD-grown monolayer graphene onto arbitrary substrates. *ACS Nano*. 2011;5:6916–6924. DOI: 10.1021/nn201207c.
- [68] Nemanich RJ, Solin SA. First- and second-order Raman scattering from finite-size crystals of graphite. *Physical Review B*. 1979;20:392–401.
- [69] Pei S, Cheng HM. The reduction of graphene oxide. *Carbon*. 2012;50:3210–3228. DOI: 10.1016/j.carbon.2011.11.010.
- [70] Suk JW, Piner RD, An J, Ruoff RS. Mechanical properties of monolayer graphene oxide. *ACS Nano*. 2010;4:6557–6564. DOI: 10.1021/nn101781v.

- [71] Marcano DC, Kosynkin DV, Berlin JM, Sinitskii A, Sun Z, Slesarev A, Alemany LB, Lu W, Tour JM. Improved synthesis of graphene oxide. *ACS Nano*. 2010;4:4806–4814. DOI: 10.1021/nn1006368.
- [72] Akhavan O, Ghaderi E. Escherichia coli bacteria reduce graphene oxide to bactericidal graphene in a self-limiting manner. *Carbon*. 2012;50:1853–1860. DOI: 10.1016/j.carbon.2011.12.035.
- [73] Guerrero-Contreras J, Caballero-Briones F. Graphene oxide powders with different oxidation degree, prepared by synthesis variations of the Hummers method. *Materials Chemistry and Physics*. 2015;153:209–220. DOI: 10.1016/j.matchemphys.2015.01.005.
- [74] Botas C, Álvarez P, Blanco C, Santamaría R, Granda M, Gutiérrez MD, Rodríguez-Reinoso F, Menéndez R. Critical temperatures in the synthesis of graphene-like materials by thermal exfoliation-reduction of graphite oxide. *Carbon*. 2013;52:476–485. DOI: 10.1016/j.carbon.2012.09.059.
- [75] Zhao W, Kido G, Hara K, Noguchi H. Characterization of neutralized graphite oxide and its use in electric double layer capacitors. *Journal of Electroanalytical Chemistry*. 2014;712:185–193. DOI: 10.1016/j.jelechem.2013.11.007.

IntechOpen